Published in final edited form as:
Microsc Res Tech. 2013 September ; 76(9): . doi:10.1002/jemt.22251.

Mesoporous Iron Oxide Nanoparticles Prepared by Polyacrylic Acid Etching and Their Application in Gene Delivery to Mesenchymal Stem Cells

BINRUI CAO, **PENGHE QIU**, and **CHUANBIN MAO***
Department of Chemistry and Biochemistry, Stephenson Life Sciences Research Center, University of Oklahoma, Norman, Oklahoma 73019

Abstract

Novel monodisperse mesoporous iron oxide nanoparticles (m-IONPs) were synthesized by a postsynthesis etching approach and characterized by electron microscopy. In this approach, solid iron oxide nanoparticles (s-IONPs) were first prepared following a solvothermal method, and then etched anisotropically by polyacrylic acid to form the mesoporous nanostructures. MTT cytotoxicity assay demonstrated that the m-IONPs have good biocompatibility with mesenchymal stem cells (MSCs). Owing to their mesoporous structure and good biocompatibility, these monodisperse m-IONPs were used as a nonviral vector for the delivery of a gene of vascular endothelial growth factor (VEGF) tagged with a green fluorescence protein (GFP) into the hard-to-transfect stem cells. Successful gene delivery and transfection were verified by detecting the GFP fluorescence from MSCs using fluorescence microscopy. Our results illustrated that the m-IONPs synthesized in this work can serve as a potential nonviral carrier in gene therapy where stem cells should be first transfected and then implanted into disease sites for disease treatment.

Keywords

postsynthesis etching; mesoporous nanostructures; iron oxide nanoparticles; gene delivery

INTRODUCTION

Gene therapy holds promise in treating cancers and genetic diseases as well as regenerating tissues; and its success relies on the delivery of specific foreign genes into target cells with the aid of a carrier (also called vector) (Friedmann, 1996; Luo and Saltzman, 2000; Roy et al., 1999; Verma and Somia, 1997; Yamada et al., 2003). There are generally two types of gene delivery carriers, namely viral and nonviral delivery vectors. The viral vectors, including retroviruses, adenovirus, and lentiviruses, can achieve high gene expression efficiency in delivering foreign genes to numerous cell lines (Anderson, 1998). However, the safety issue due to their toxicity and immunogenicity is a main concern in their clinical applications. On the other hand, nonviral delivery vectors, such as cationic lipids, peptides, polymers, and dendrimers (Mintzer and Simanek, 2009), showed some advantages in reducing the risk of cytotoxicity and immunogenicity (Carter and Samulski, 2000; Pouton and Seymour, 2001). Nevertheless, their transfection efficiency is low, which limits their uses in gene therapy. Magnetic iron oxide nanoparticles, such as magnetite (Fe_3O_4) nanoparticles, are proposed to be one of the ideal nonviral vectors due to their

*Correspondence to: Chuanbin Mao, Department of Chemistry and Biochemistry, Stephenson Life Sciences Research Center, University of Oklahoma, Norman, Oklahoma 73019. cbmao@ou.edu.

biocompatibility (Frey et al., 2009; Shubayev et al., 2009; Sun et al., 2008; Veiseh et al., 2010). Their magnetic properties enable the use of an external magnetic field to guide them to deliver the foreign gene to target cells and achieve enhanced transfection through a mechanism called magnetic targeting (Akiyama et al., 2010; Namgung et al., 2010; Song et al., 2010). Mesoporous materials are a type of material containing pores with diameters between 2 and 50 nm. Their porous structure enables high loading/encapsulation of desired gene fragments to target cells and achieve enhanced transfection (Slowing and others, 2008). Here, we report a novel strategy to prepare mesoporous iron oxide nanoparticles (m-IONPs) based on a postsynthesis etching approach. In this approach, solid iron oxide nanoparticles (s-IONPs) were first prepared using a solvothermal method, and then etched anisotropically by polyacrylic acid to form the mesoporous nanostructures. The as-prepared m-IONPs are shown to be biocompatible and serve as an efficient nonviral vector for gene delivery to stem cells. Stem cells are hard to transfect and thus we use mesenchymal stem cells (MSCs) as target cells to demonstrate the successful use of m-IONPs in carrying DNA. Furthermore, vascular endothelial growth factor (VEGF) is a protein that can induce blood vessel formation (e.g., angiogenesis). Therefore, we used a plasmid DNA encoding VEGF tagged with an enhanced green fluorescence protein (EGFP) as a model gene to test the gene delivery by m-IONPs.

MATERIALS AND METHODS

Materials

$FeCl_3 \cdot 6H_2O$ (≥99.0%), anhydrous sodium acetate (NaAc≥ 99.0%), polyvinylpyrrolidone (PVP, M_w = 29,000), poly(acrylic acid) (PAA, $M_w \approx 1800$), polyethylenimine (branched PEI; average M_W = 25,000), ethylene glycol (EG), diethylene glycol (DEG), and ethanol were purchased from Sigma–Aldrich. All chemicals were of analytical grade and used as received without further purification. Phosphate buffered saline (PBS, 0.01M, pH 7.4) solution was prepared according to the documented procedures. Deionized water was obtained from a Milli-Q water system.

Solvothermal Synthesis of s-IONPs

s-IONPs were synthesized using a solvothermal method. Generally, under vigorous stirring, ferric chloride (20 mmol), sodium acetate (40 mmol) and PVP (1.5 g) were added sequentially into 40 ml of EG to form a clear solution, which was then transferred to a Teflon-lined stainless steel autoclave (50 ml capacity). The autoclave was heated and maintained at 200°C for 10 h. Afterward, the IONPs were collected by centrifugation, washed, and dried for further use.

Preparation of m-IONPs Through Polyacrylic Acid Etching

The as-prepared s-IONPs (10 mg) were first resuspended into 2 ml of DEG, followed by mixing with a hot PAA solution (0.5 g in 8 ml of DEG). The mixture was then heated under 240°C for 2 h, allowing the as-prepared s-IONPs to become partially dissolved by PAA to form the mesoporous structure. The resultant m-IONPs were collected, washed and redispersed into a basic aqueous solution.

For gene delivery experiments, the PAA stabilized m-IONPs were coated with another layer of PEI through electrostatic interaction between PAA and PEI. The PEI coating was achieved by simply mixing 1 ml of the as-prepared m-IONPs suspension with 5 ml of 1 wt% PEI solution and sonicating for 30 min. The PEI stabilized m-IONPs were then collected by a magnet and redispersed into PBS.

Loading of Plasmid DNA Onto the m-IONPs

The plasmid DNA (pEGFP-kozVEGF 165), which encodes VEGF tagged with EGFP, was dissolved in PBS buffer at a concentration of 750 μg ml^{-1}. To load DNA into the m-IONPs, 0.1 ml of plasmid DNA was mixed with 0.2 ml m-IONPs (m-IONPs to DNA mass ratio in between 0.5 and 5) of varying concentrations and the mixture was shaken for 2 days under 4°C. Afterwards, the m-IONPs were collected by a magnet and redispersed into PBS. The successful loading of DNA into m-IONPs was verified by a gel retardation assay, where 10 μl of the DNA-loaded m-IONPs was used to run the electrophoresis in a 1% agarose gel (130V) with ethidium bromide staining. The images were taken on a Bio-Rad Gel Imaging System.

Cell Viability Assay

Rat MSCs (rMSCs) were plated at a density of 4×10^3 cells/well in 96-well plates in the standard growth medium for 24 h. Then, they were treated with medium without fetal bovine serum (FBS) but containing m-IONPs. After 4-h incubation, the medium was removed and cells were then cultured in medium containing FBS for another 24 h. The measurement of cell viability was carried out using a standard 3-(4,5-dimethyl thiazol-2-yl)–2,5-diphenyl tetrazolium bromide (MTT) assay.

Gene Transfection in rMSCs

rMSCs were cultured as described in our earlier publication (Zhu et al., 2011). The cells at a density of 1×10^4cells/well in a 24-well plate were treated with a culture medium containing DNA-loaded m-IONPs (with a m-IONPs/DNA mass ratio of 0.5 or 5) and incubated for 4 h. Then the medium was changed to a medium containing FBS. A fluorescence microscope was used to verify the transfection of the cells by the m-IONPs. Transfection by naked DNA was also performed as controls.

RESULTS

The size and morphology of the as-synthesized and PAA etched IONPs were first studied by the TEM and SEM (Fig. 1). It can be seen that the as-synthesized IONPs (i.e., s-IONPs) are very uniform in size, and their average diameter is about 200 nm (Figs. 1A and 1B). There are a few pores on some of the s-IONPs. The IONPs remained spherical after PAA etching, but they showed a totally different morphology under the SEM. The surface of IONPs became significantly roughened after the etching (Fig. 1C), indicating that iron oxide has been partially dissolved by the weak acidic polymer at a high temperature (240°C). This could also be confirmed by the TEM images, which show the presence of small particle debris and incomplete IONPs (Fig. 1D, indicated by arrows). At a higher magnification, numerous tiny pores are clearly visible on the etched IONPs whereas they are not obvious on the s-IONPs (insets in Figs. 1B and 1D). For this reason, the PAA etched IONPs are named here as mesoporous IONPs (m-IONPs). The crystal structure of the s-IONPs was studied by the powder X-ray diffraction (XRD). The XRD pattern (Fig. 2) suggests that the as-synthesized s-IONPs are of cubic magnetite (Fe_3O_4). The porosity of m-IONPs was studied by measuring nitrogen adsorption–desorption isotherms and Barrett–Joyner–Halenda (BJH) pore size distribution curve (Fig. 3). The N_2 adsorption–desorption isotherm exhibits a type IV behavior with an apparent hysteresis loop in the range 0.5–1.0 P/P_0, indicating the presence of mesoporous structures in the prepared m-IONPs. The pore size distribution curve (Fig. 3, inset) shows that there is a dominant peak around 18.0 nm, further demonstrating that these m-IONPs are indeed mesoporous. The magnetic properties of the s-IONPs and m-IONPs were measured by a superconducting quantum interference device (SQUID) magnetometer. The measurement was made at 300 K with magnetic field sweeping between −10 and 10 kOe. As can be seen from the hysteresis loop in Figure 4, the

s-IONPs showed weak ferromagnetism behavior with a coercivity of 35 Oe, a remanence of 2.8 emu g^{-1} and a saturation magnetization of 86.6 emu g^{-1} under room temperature. For the m-IONPs, their hysteresis loop is not significantly different from that of the s-IONPs, except that the saturation magnetization has dropped to 75.4 emu g^{-1}.

To facilitate gene uptake, the PAA stabilized m-IONPs were coated with another layer of positively charged biocompatible polymer (PEI). The success of PEI coating onto the m-IONPs was confirmed by the fact that the zeta potential of the nanoparticles was changed from −33.97 to 20.76 mV before and after coating. The biocompatibility of the PEI coated m-IONPs was evaluated by the MTT cytotoxicity assay. After coculturing with the m-IONPs (ranging from 1 to 100 μg ml^{-1}) for 72 h, the rMSCs showed no remarkable difference in proliferation and viability in comparison to those cultured without nanoparticles (Fig. 5). The MTT assay results demonstrated that the m-IONPs are biocompatible and suitable for further use as a nonviral vector for gene delivery.

The complex of the plasmid DNA with m-IONPs was formed by simply mixing and gently shaking the two species. To identify the highest DNA loading efficiency, different mass ratios of m-IONPs to DNA, including 0.5, 1.25, 2.5, and 5, were practiced and examined by a gel retardation assay. In this assay, unbound DNA is free to move and penetrate into the gel under the applied electric field, while DNA bound to the m-IONPs will be retarded at the starting point. Thus, by finding whether there is a band corresponding to the free DNA, one can determine the optimized m-IONPs to DNA mass ratios that can make DNA loaded onto the nanoparticles with the highest loading efficiency. In Figure 6, a free DNA band was observed at the mass ratios of 0.5, 1.25, and 2.5 but not at the mass ratio of 5. This fact suggests that at the ratio of 5 the DNA had been completely loaded into the m-IONPs. Hence, the m-IONPs to DNA mass ratio of 5 is considered to be the optimized ratio for DNA loading under the experimental conditions.

After successfully loading the plasmid DNA (pEGFP-kozVEGF165), the m-IONPs were tested for their effectiveness in the gene transfection. The gene transfection experiment was conducted in rMSCs by treating the same number of rMSCs with plasmid DNA either alone or carried by nanoparticles. A fluorescence microscope was used to assess the effectiveness of the m-IONPs DNA vectors as successful expression of pEGFP-kozVEGF165 plasmid DNA expression inside the cells will result in the production of a GFP marker protein fused to VEGF. As shown in Figure 7A, no green fluorescence was observed in cells cultured with naked DNA, indicating that without a suitable delivery vector, the plasmid DNA alone cannot be delivered to the cells and expressed. However, when m-IONPs were used as a carrier, the transfection of rMSCs occurred (Figs. 7B and 7C). Moreover, only a low percentage of cells exhibited fluorescence when m-IONPs/DNA complex having a mass ratio of 0.5 was employed for the transfection (Fig. 7B), while under a mass ratio of 5, more cells showed green fluorescence (Fig. 7C). Our data show that m-IONPs can load DNA at a reasonably high efficiency and further transfect rMSCs successfully.

DISCUSSION

Postsynthesis etching has been an important method to prepare nanoparticles with structures that are usually hard to obtain through direct chemical synthesis. Such etching based approach involves chemical removal of a portion of material in the presynthesized nanoparticles. Chemical etching has been applied to both heterogeneous and homogeneous (not including alloy) nanoparticles to prepare various nanostructures. In heterogeneous nanoparticles, the etching reagent is chosen to be reactive only with the component to be removed (Zeng et al., 2008); while in homogeneous nanoparticles, chemicals of low activity are usually employed to achieve anisotropic dissolution of the material (Hu et al., 2012;

Mulvihill et al., 2010; Wong et al., 2011; Zhao et al., 2010). In the current work, the m-IONPs were produced as a result of heat treatment of the as-prepared s-IONPs in DEG in the presence of PAA. We believe there are two factors that lead to the formation of mesoporous nanostructures during the heat treatment. First, just like the behavior of most weak acids in organic solvents, the carboxyl group of PAA can partially dissociate in DEG, at a high temperature, to generate hydrogen ions (Lin and Hsieh, 1977; Lin and Yu, 1978), which caused slow chemical etching of the nanoparticles through reaction between the weak acid and iron oxide. Second, the surface of IONPs is protected densely by PAA as a result of strong chelation between the carboxyl groups and iron atoms. And such slow, protected etching of inorganic oxides nanoparticles has been reported to take place in an anisotropic manner (rather than isotropic), leading to the formation of the mesoporous structures (Zhang et al., 2008).

In the biological research, nanosized particles of polymers, lipids and many inorganic materials have been actively employed for drug and gene delivery. As drug/gene carriers, the nanoparticles have their advantages in several aspects. First, the nanoparticles are tiny and stable in the physiological environment; as a result, they have relatively long blood circulation time, and therefore the tissue uptake of drugs is enhanced (Moghimi et al., 2001; von Maltzahn et al., 2009). Second, the surface chemistry of nanoparticles can be engineered as demanded. For example, some tissue targeting motifs, like antibodies and peptides can be linked onto the surface of nanoparticles through chemical conjugation to achieve specified drug and gene delivery (Gupta and Gupta, 2005; Mout et al., 2012; Sperling and Parak, 2010). Finally, through careful design of the nanoparticle structures, controllable release of molecules can be achieved (Giri et al., 2005; Slowing et al., 2008; Trewyn et al., 2004). As carriers, the nanoparticle structures can significantly affect the loading efficiency of molecules. For this reason, nanoparticles of large surface areas, such as hollow, mesoporous and dendritic nanoparticles, are always preferred over the solid nanoparticles in the drug and gene delivery (Amstad and Reimhult, 2012; He and Shi, 2011; Shin et al., 2009; Son et al., 2007a,b; Stover and others, 2008; Wu et al., 2011). For mesoporous nanoparticles, such as m-IONPs in this work, the molecules can not only be loaded onto their outer surface, but also into the inner cavities, thus the loading efficiency can be greatly increased. Consequently, when the gene-loaded m-IONPs were delivered into cells, good transfection efficiency was obtained.

Although a GFP marker is fused to VEGF protein in Figure 7 for easy confirmation of transfection using fluorescence microscopy (Fig. 7C), this work shows the use of a non-viral vector in the delivery of an important functional gene that encodes VEGF. Stem cells carrying VEGF gene can express VEGF, which can induce blood vessel formation *in vivo*. Therefore, this work may provide a new non-viral vector that can be potentially applied in the stem cell-based gene therapy, where angiogenesis is needed for treating diseases such as myocardial ischemia or regenerating vascularized issue such as bone. In such gene therapy, stem cells can be first transfected by the VEGF-gene-loaded m-IONPs and then implanted into disease sites. They are expected to perform two important functions: producing VEGF protein and differentiation into functional cells such as heart muscle cells for treating myocardial ischemia or bone forming cells for regenerating vascularized bone tissue.

CONCLUSIONS

In conclusion, we have prepared monodisperse m-IONPs through a postsynthesis etching approach. The etching was taken place by heating the as-synthesized s-IONPs in the diethylene glycol solution of polyarylic acid. During the heat treatment, the nanoparticles were etched anisotropically to form the mesoporous structure. The crystallinity and magnetic properties of the IONPs were verified by XRD and SQUID respectively. The m-

IONPs have also shown very good biocompatibility and can be efficiently loaded with plasmid DNA with the aid of PEI due to their porous structures. The DNA was then successfully delivered into cells to achieve successful transfection of the hard-to-transfect stem cells. Our work demonstrated that the m-IONPs formed through the postsynthesis etching method can be potentially used as a non-viral vector for DNA delivery in stem cell-based gene therapy.

Acknowledgments

Contract grant sponsor: National Science Foundation; Contract grant numbers: CBET-0854465, CBET-0854414, DMR-0847758; Contract grant sponsors: National Institutes of Health; Contract grant numbers: 5R01HL092526-02, 1R21EB015190-01A1, 4R03AR056848-03; Contract grant sponsors: Department of Defense Peer Reviewed Medical Research Program; Contract grant number: W81XWH-12-1-0384; Contract grant sponsor: Oklahoma Center for the Advancement of Science and Technology; Contract grant number: HR11-006; Contract grant sponsor: Oklahoma Center for Adult Stem Cell Research; Contract grant number: 434003.

The authors thank Drs. Ziwei Deng, Haibao Zhu, and Andrew S. Madden for their help during experiments.

References

Akiyama H, Ito A, Kawabe Y, Kamihira M. Genetically engineered angiogenic cell sheets using magnetic force-based gene delivery and tissue fabrication techniques. Biomaterials. 2010; 31:1251–1259. [PubMed: 19942286]

Amstad E, Reimhult E. Nanoparticle actuated hollow drug delivery vehicles. Nanomedicine. 2012; 7:145–164. [PubMed: 22191783]

Anderson WF. Human gene therapy. Nature. 1998; 392:25–30. [PubMed: 9579858]

Carter PJ, Samulski RJ. Adeno-associated viral vectors as gene delivery vehicles. Int J Mol Med. 2000; 6:17–27. [PubMed: 10851261]

Frey NA, Peng S, Cheng K, Sun SH. Magnetic nanoparticles: Synthesis, functionalization, and applications in bioimaging and magnetic energy storage. Chem Soc Rev. 2009; 38:2532–2542. [PubMed: 19690734]

Friedmann T. Human gene therapy—An immature genie, but certainly out of the bottle. Nat Med. 1996; 2:144–147. [PubMed: 8574951]

Giri S, Trewyn BG, Stellmaker MP, Lin VSY. Stimuli-responsive controlled-release delivery system based on mesoporous silica nanorods capped with magnetic nanoparticles. Angew Chem Int Ed. 2005; 44:5038–5044.

Gupta AK, Gupta M. Synthesis and surface engineering of iron oxide nanoparticles for biomedical applications. Biomaterials. 2005; 26:3995–4021. [PubMed: 15626447]

He QJ, Shi JL. Mesoporous silica nanoparticle based nano drug delivery systems: Synthesis, controlled drug release and delivery, pharmacokinetics and biocompatibility. J Mater Chem. 2011; 21:5845–5855.

Hu M, Furukawa S, Ohtani R, Sukegawa H, Nemoto Y, Reboul J, Kitagawa S, Yamauchi Y. Synthesis of Prussian blue nanoparticles with a hollow interior by controlled chemical etching. Angew Chem Int Ed. 2012; 51:984–988.

Lin CC, Hsieh KH. Kinetics of polyesterification. 1. Adipic acid and ethylene-glycol. J Appl Polym Sci. 1977; 21:2711–2719.

Lin CC, Yu PC. Kinetics of polyesterification. 2. Succinic acid and ethylene-glycol. J Polym Sci A Polym Chem. 1978; 16:1005–1016.

Luo D, Saltzman WM. Synthetic DNA delivery systems. Nat Biotechnol. 2000; 18:33–37. [PubMed: 10625387]

Mintzer MA, Simanek EE. Nonviral vectors for gene delivery. Chem Rev. 2009; 109:259–302. [PubMed: 19053809]

Moghimi SM, Hunter AC, Murray JC. Long-circulating and target-specific nanoparticles: Theory to practice. Pharmacol Rev. 2001; 53:283–318. [PubMed: 11356986]

Mout R, Moyano DF, Rana S, Rotello VM. Surface functionalization of nanoparticles for nanomedicine. Chem Soc Rev. 2012; 41:2539–2544. [PubMed: 22310807]

Mulvihill MJ, Ling XY, Henzie J, Yang PD. Anisotropic etching of silver nanoparticles for plasmonic structures capable of single-particle SERS. J Am Chem Soc. 2010; 132:268–274. [PubMed: 20000421]

Namgung R, Singha K, Yu MK, Jon S, Kim YS, Ahn Y, Park IK, Kim WJ. Hybrid superparamagnetic iron oxide nanoparticle-branched polyethylenimine magnetoplexes for gene transfection of vascular endothelial cells. Biomaterials. 2010; 31:4204–4213. [PubMed: 20170956]

Pouton CW, Seymour LW. Key issues in non-viral gene delivery. Adv Drug Deliv Rev. 2001; 46:187–203. [PubMed: 11259840]

Roy K, Mao HQ, Huang SK, Leong KW. Oral gene delivery with chitosan-DNA nanoparticles generates immunologic protection in a murine model of peanut allergy. Nat Med. 1999; 5:387–391. [PubMed: 10202926]

Shin JM, Anisur RM, Ko MK, Im GH, Lee JH, Lee IS. Hollow manganese oxide nanoparticles as multifunctional agents for magnetic resonance imaging and drug delivery. Angew Chem Int Ed. 2009; 48:321–324.

Shubayev VI, Pisanic TR, Jin SH. Magnetic nanoparticles for theragnostics. Adv Drug Deliv Rev. 2009; 61:467–477. [PubMed: 19389434]

Slowing II, Vivero-Escoto JL, Wu CW, Lin VSY. Mesoporous silica nanoparticles as controlled release drug delivery and gene transfection carriers. Adv Drug Deliv Rev. 2008; 60:1278–1288. [PubMed: 18514969]

Son SJ, Bai X, Lee S. Inorganic hollow nanoparticles and nanotubes in nanomedicine. Part 2: Imaging, diagnostic, and therapeutic applications. Drug Discov Today. 2007a; 12:657–663. [PubMed: 17706548]

Son SJ, Bai X, Lee SB. Inorganic hollow nanoparticles and nanotubes in nanomedicine. Part 1. Drug/gene delivery applications. Drug Discov Today. 2007b; 12:650–656. [PubMed: 17706547]

Song HP, Yang JY, Lo SL, Wang Y, Fan WM, Tang XS, Xue JM, Wang S. Gene transfer using self-assembled ternary complexes of cationic magnetic nanoparticles, plasmid DNA and cell-penetrating Tat peptide. Biomaterials. 2010; 31:769–778. [PubMed: 19819012]

Sperling RA, Parak WJ. Surface modification, functionalization and bioconjugation of colloidal inorganic nanoparticles. Philos Trans R Soc A Math Phys Eng Sci. 2010; 368:1333–1383.

Stover TC, Kim YS, Lowe TL, Kester M. Thermoresponsive and biodegradable linear-dendritic nanoparticles for targeted and sustained release of a pro-apoptotic drug. Biomaterials. 2008; 29:359–369. [PubMed: 17964645]

Sun C, Lee JSH, Zhang MQ. Magnetic nanoparticles in MR imaging and drug delivery. Adv Drug Deliv Rev. 2008; 60:1252–1265. [PubMed: 18558452]

Trewyn BG, Whitman CM, Lin VSY. Morphological control of room-temperature ionic liquid templated mesoporous silica nanoparticles for controlled release of antibacterial agents. Nano Lett. 2004; 4:2139–2143.

Veiseh O, Gunn JW, Zhang MQ. Design and fabrication of magnetic nanoparticles for targeted drug delivery and imaging. Adv Drug Deliv Rev. 2010; 62:284–304. [PubMed: 19909778]

Verma IM, Somia N. Gene therapy—Promises, problems and prospects. Nature. 1997; 389:239–242. [PubMed: 9305836]

von Maltzahn G, Park JH, Agrawal A, Bandaru NK, Das SK, Sailor MJ, Bhatia SN. Computationally guided photothermal tumor therapy using long-circulating gold nanorod antennas. Cancer Res. 2009; 69:3892–3900. [PubMed: 19366797]

Wong YJ, Zhu LF, Teo WS, Tan YW, Yang YH, Wang C, Chen HY. Revisiting the stober method: In homogeneity in silica shells. J Am Chem Soc. 2011; 133:11422–11425. [PubMed: 21732677]

Wu XM, He XH, Zhong L, Lin SL, Wang DL, Zhu XY, Yan DY. Water-soluble dendritic-linear triblock copolymer-modified magnetic nanoparticles: Preparation, characterization and drug release properties. J Mater Chem. 2011; 21:13611–13620.

Yamada T, Iwasaki Y, Tada H, Iwabuki H, Chuah MKL, VandenDriessche T, Fukuda H, Kondo A, Ueda M, Seno M, Tanizawa K, Kuroda S. Nanoparticles for the delivery of genes and drugs to human hepatocytes. Nat Biotechnol. 2003; 21:885–890. [PubMed: 12833071]

Zeng HB, Cai WP, Liu PS, Xu XX, Zhou HJ, Klingshirn C, Kalt H. ZnO-based hollow nanoparticles by selective etching: Elimination and reconstruction of metal-semiconductor interface, improvement of blue emission and photocatalysis. Acs Nano. 2008; 2:1661–1670. [PubMed: 19206370]

Zhang Q, Zhang TR, Ge JP, Yin YD. Permeable silica shell through surface-protected etching. Nano Lett. 2008; 8:2867–2871. [PubMed: 18698725]

Zhao L, Zhao YF, Han Y. Pore fabrication in various silica-based nanoparticles by controlled etching. Langmuir. 2010; 26:11784–11789. [PubMed: 20557087]

Zhu H, Cao B, Zhen Z, Laxmi A, Li D, Liu S, Mao CB. Controlled growth and differentiation of MSCs on grooved films assembled from monodisperse biological nanofibers with genetically tunable surface chemistries. Biomaterials. 2011; 32:4744–4752. [PubMed: 21507480]

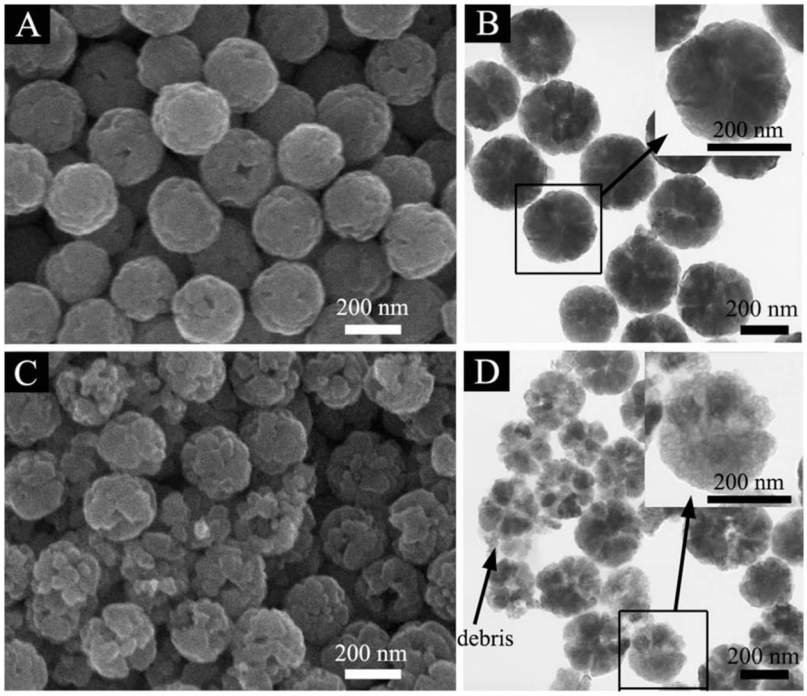

Fig. 1.

SEM (**A**,**C**) and TEM (**B**,**D**) images of IONPs. (A,B) As-synthesized s-IONPs; (C,D) m-IONPs, produced by PAA etching of the s-IONPs. Insets in B and D, higher magnification of a typical nanoparticle showing the difference in porosity before and after PAA etch. Left arrow in D indicates nanoparticles debris formed during the etching process.

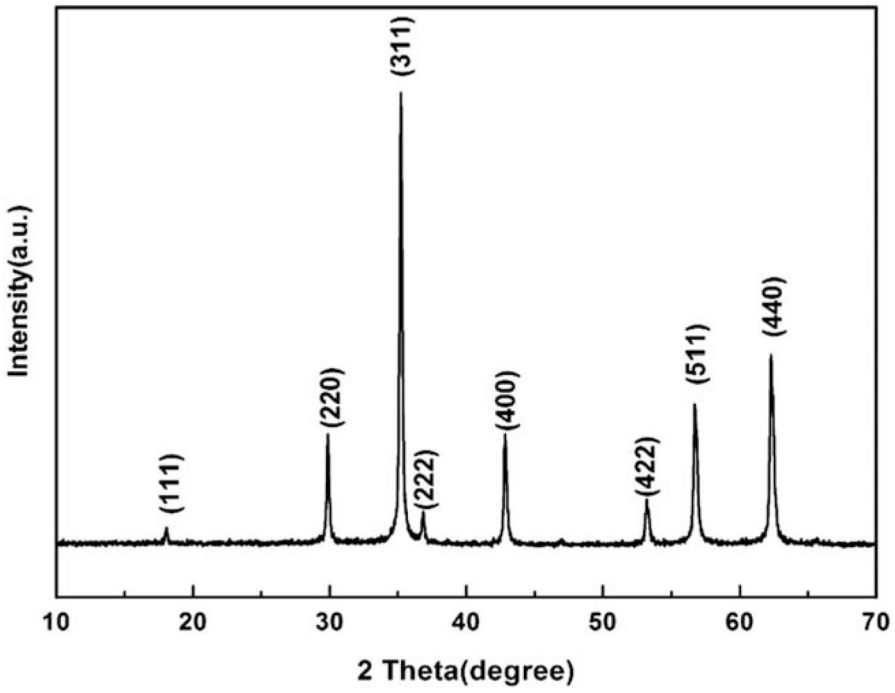

Fig. 2.
XRD pattern of m-IONPs that can be indexed by JCPDS #75-0033.

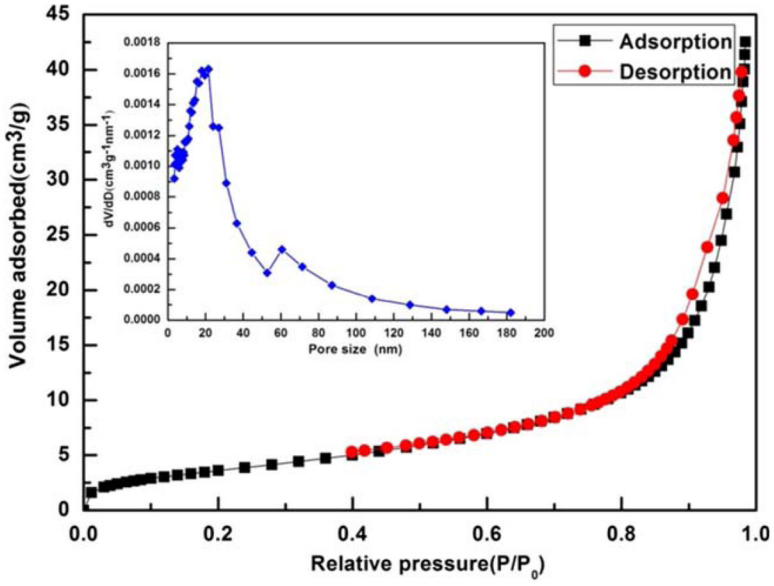

Fig. 3.

The nitrogen adsorption–desorption isotherm and Barrett-Joyner-Halenda (BJH) pore size distribution curves (inset) of m-IONPs. [Color figure can be viewed in the online issue, which is available at wileyonlinelibrary.com.]

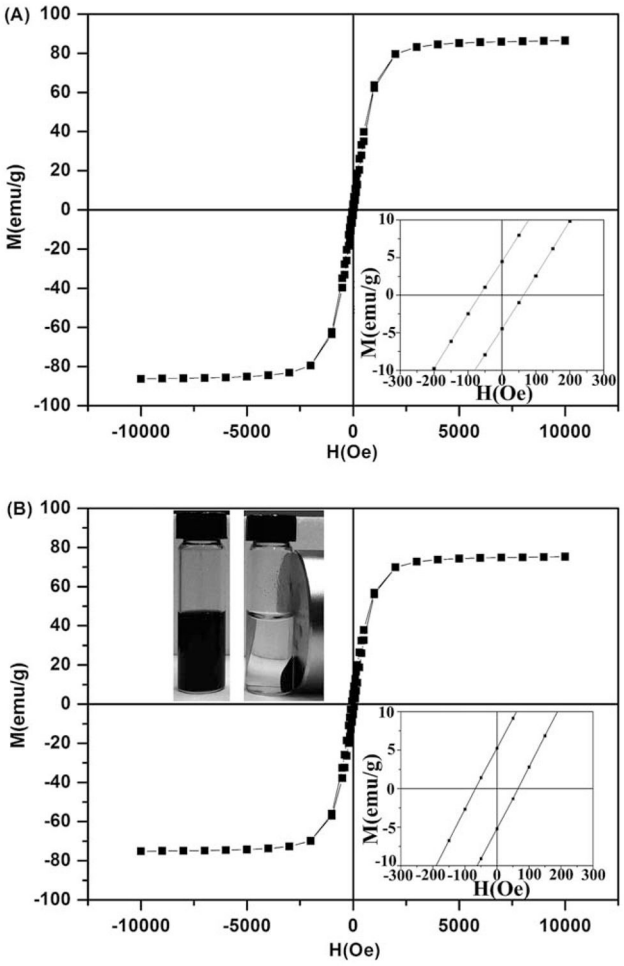

Fig. 4.

Room temperature hysteresis curves of (**A**) s-IONPs and (**B**) m-IONPs. The enlarged hysteresis curves around zero field with a scale from −300 to 300 Oe are depicted as the lower right insets in (A) and (B). The photograph (the upper left inset in B) shows a suspension of m-IONPs dispersed in water before (left) and after (right) being placed around a magnet.

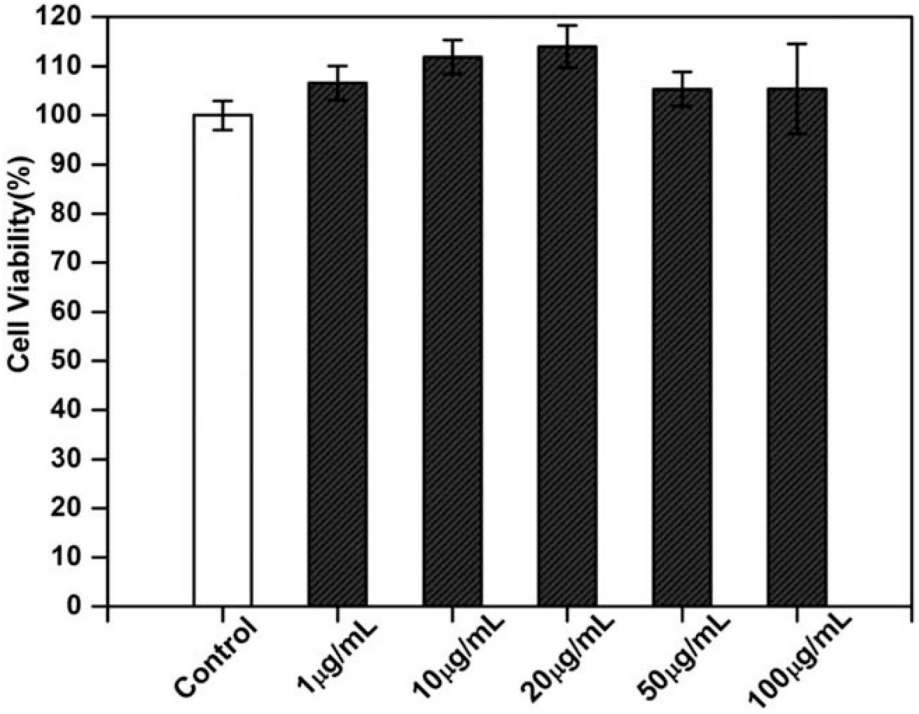

Fig. 5.

Cytotoxicity study of m-IONPs by MTT assays. MSCs were cultured for 72 h in the medium containing m-IONPs with a concentration ranging from 1 to 100 μg ml^{-1}.

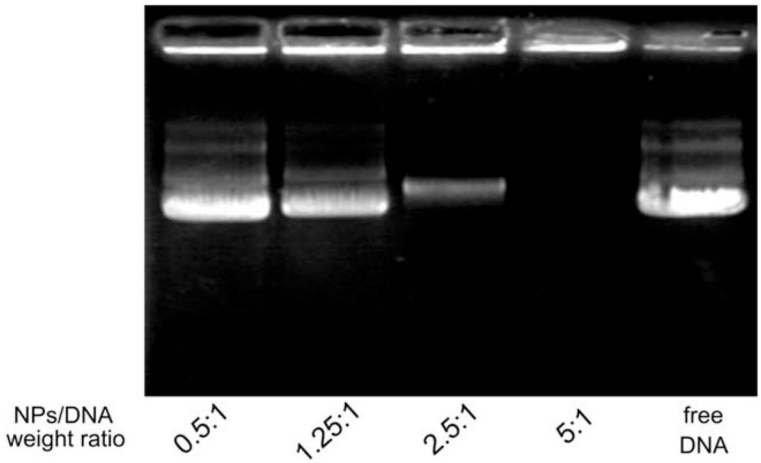

Fig. 6.
Gel retardation assay of m-IONPs loaded with plasmid DNA at different nanoparticles/DNA weight ratios.

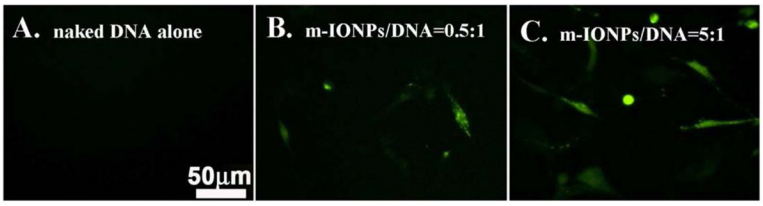

Fig. 7.

Fluorescence microscopy study of gene transfection in rMSCs. (**A**) Transfection by naked plasmid DNA alone; (**B** and **C**) Transfection by plasmid DNA loaded onto m-IONPs at a weight ratio of 0.5:1 (B) and 5:1 (C). The scale bar applies to all images. [Color figure can be viewed in the online issue, which is available at wileyonlinelibrary.com.]